Amino Acids (2012) 43:1625–1632
DOI 10.1007/s00726-012-1238-6

ORIGINAL ARTICLE

Evaluation of fluorine-labeled gastrin-releasing peptide receptor (GRPR) agonists and antagonists by LC/MS

Ying Ma · Min Yang · Haokao Gao · Gang Niu · Yongjun Yan · Lixin Lang · Dale O. Kiesewetter · Xiaoyuan Chen

Received: 26 October 2011 / Accepted: 31 January 2012 / Published online: 22 February 2012

Abstract An LC/MS method was used to evaluate 2-fluoropropionyl (FP) and 4-fluorobenzoyl (FB) modified bombsin peptides: GRPR agonist [Aca-QWAVGHLM-NH_2] and antagonist [fQWAVGHL-NHEt], and their hydrophilic linker modified counterparts with the attachment of GGGRDN sequence. This study developed strategies to evaluate the in vitro receptor mediated cell uptake and metabolic profile of the various GRPR agonists and antagonists. We identified the metabolites produced by rat hepatocytes and quantitatively analyzed the uptake and internalization of the ligands in PC-3 human prostate cancer cells. The major metabolites of both GRPR agonists and antagonists were the result of peptide bond hydrolysis between WA and AV. The agonists also formed a unique metabolite resulting from hydrolysis of the C-terminal amide. The antagonists showed significantly higher stability against metabolism compared to the agonists in rat hepatocytes. The directly modified agonists (FP-BBN and FB-BBN) had higher internalization with similar cell binding compared to the unmodified agonist (BBN), whereas the hydrophilic linker modified agonists (G-BBN and FG-BBN) had much lower total cell uptake. The labeled antagonists (FP-NBBN, FB-NBBN, G-NBBN and FP-G-NBBN) displayed lower internalization. The optimal imaging agent will depend on the interplay of ligand metabolism, cellular uptake, and internalization in vivo.

Keywords LC/MS · Gastrin releasing peptide receptor (GRPR) · Bombesin (BBN) · Agonist · Antagonist · PET

Introduction

The gastrin-releasing peptide receptor (GRPR) is an important target for cancer imaging and therapy since overexpression of GRPR is related to proliferation and growth of human cancers from a variety of origins, including breast, lung, pancreatic, and prostate (Fleischmann et al. 2005; Fleischmann et al. 2007; Markwalder and Reubi 1999; Reubi et al. 2004; Sun et al. 2000). Both GRPR agonists and antagonists have been developed as therapeutic agents (Abd-Elgaliel et al. 2008; Abiraj et al. 2010; Ananias et al. 2011; Cescato et al. 2008; Mansi et al. 2009; Reubi et al. 2004; Schroeder et al. 2009; Smith et al. 2005). Molecular imaging of GRPR has also been explored to determine the presence, concentration, and therapeutic efficacy in various tumor types (Cornelio et al. 2007a; Cornelio et al. 2007b; Gugger and Reubi 1999; Markwalder and Reubi 1999; Smith et al. 2005). An optimal radiotracer for GRPR should meet several criteria. Firstly, the ligand must display high affinity for GRPR and demonstrate specific tumor uptake. Secondly, it must exhibit ideal

Y. Ma and M. Yang contributed equally in this work.

Y. Ma · M. Yang · H. Gao · G. Niu · Y. Yan · L. Lang · D. O. Kiesewetter · X. Chen (✉)
Laboratory of Molecular Imaging and Nanomedicine (LOMIN), National Institute of Biomedical Imaging and Bioengineering (NIBIB), National Institutes of Health (NIH), 31 Center Dr, Suite 1C14, Bethesda, MD 20892-2281, USA
e-mail: shawn.chen@nih.gov

M. Yang
Key Laboratory of Nuclear Medicine, Ministry of Health, Jiangsu Key Laboratory of Molecular Nuclear Medicine, Jiangsu Institute of Nuclear Medicine, Wuxi 214063, Jiangsu, China

D. O. Kiesewetter (✉)
National Institute of Biomedical Imaging and Bioengineering (NIBIB), National Institutes of Health (NIH), 10 Center Drive MSC 1180, Bethesda, MD 20892, USA
e-mail: dk7k@nih.gov

pharmacokinetic properties and high enough metabolic stability so that images provide high target to background ratios and contain quantitative information (Yan et al. 2010; Yang et al. 2011). Using LC/MS, the pharmacokinetics and metabolic properties of potential imaging probes can be evaluated without the need to conduct radiolabeling (Gu et al. 2011; Ma et al. 2009). In addition, LC/MS could provide the structural information of metabolism as well.

We and others have evaluated a number of radiolabeled BBN peptide derivatives for positron emission tomography (PET) imaging of GRPR expressing tumors (Chen et al. 2004b; Linder et al. 2009; Liu et al. 2009a; Liu et al. 2009c; Nock et al. 2003; Shi et al. 2008; Yan et al. 2010; Yang et al. 2011; Yang et al. 2006; Zhang et al. 2006). However, imaging with BBN analogs always suffered with low signal to noise ratios, which may result from the poor metabolic stability of the peptides. Indeed, it has been found that BBN derivatives, especially agonists, were stable over time in human plasma, but degraded rapidly in kidney and liver homogenates (Linder et al. 2009; Shipp et al. 1991; Zhang et al. 2004).

BBN analogs displayed either agonist properties or antagonist properties and efficient internalization was predominantly observed for the agonists (Wagner 1979). However, high-affinity receptor antagonists, which showed poor internalization into tumor cells, performed equally or even better in terms of in vivo uptake in animal tumor models than the corresponding agonists (Abd-Elgaliel et al. 2008; Abiraj et al. 2010; Cescato et al. 2008; Mansi et al. 2009; Schroeder et al. 2009). Thus, a comprehensive evaluation of BBN analogs requires determination of several aspects including cellular uptake, internalization, and metabolism.

We had applied LC/MS to evaluate the in vitro receptor mediated cell uptake and metabolic profile of a potent BBN agonist (Aca-QWAVGHLM-NH_2, denoted as BBN), a comparably potent BBN antagonist (fQWAVGHL-NHEt, denoted as NBBN) (Gu et al. 2011). The goal of this study was to apply the LC/MS method to evaluate variously modified BBN agonists and antagonists (Fig. 1), including those that have been modified with fluorine-containing prosthetic groups, in rat hepatocytes and PC-3 human prostate cancer cells. These results could provide guidance to develop GRPR imaging agents with improved tumor targeting and metabolic stability and to screen candidate radiotracers without the need for radiolabeled compounds.

Methods

Chemicals, reagents, and solutions

Acetonitrile (CH_3CN, HPLC grade) was purchased from Fisher Scientific (Pittsburgh, PA). All other reagents for synthesis and analysis were purchased from Sigma-Aldrich (St. Louis, MO), unless otherwise indicated. Aca-QWAVGHLM-NH_2 (BBN) and fQWAVGHL-NHEt (NBBN) were prepared according to the published procedure (Yang et al. 2011). GGGRDN-QWAVGHLM-NH_2 and GGGRDN-fQWAVGHL-NHEt were synthesised in our laboratory using solid-phase Fmoc chemistry and purified by semipreparative reversed-phase HPLC. Identity and purity were established by LC/MS: Aca-QWAVGHLM-NH_2 (m/z 1053.6 $[M + H]^+$, 95% purity), fQWAVGHL-NHEt (m/z 984.6 $[M + H]^+$, 97% purity), GGGRDN-QWAVGHLM-NH_2 (m/z 1497.1 $[M + H]^+$, 93% purity), and GGGRDN-fQWAVGHL-NHEthyl(m/z 1541.1 $[M + H]^+$, 90% purity). 2-Fluoropropionate (FP) and 4-fluorobenzoate (FB) analogs of the four peptides were prepared using the standard methods (Chen et al. 2004b; Liu et al. 2009a) (Yan et al. 2010) and purified by semipreparative reversed-phase

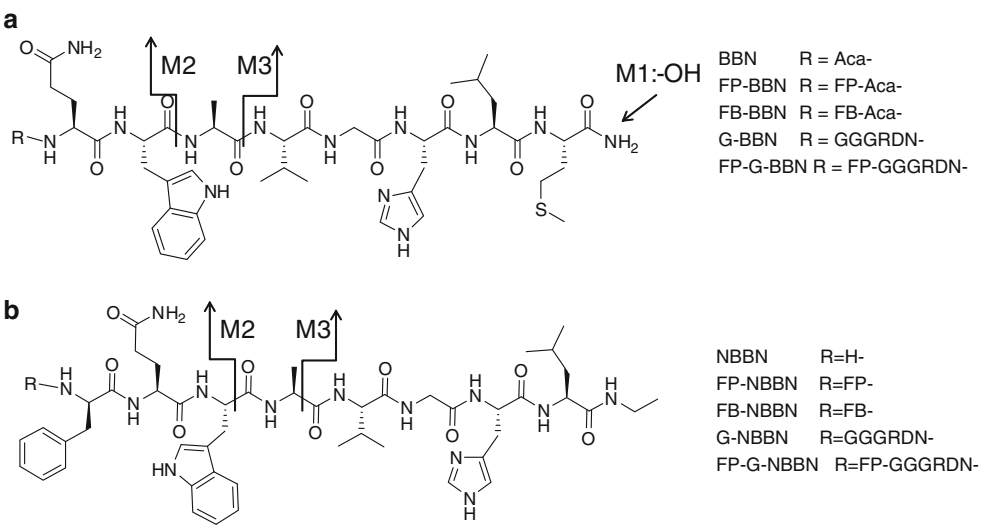

Fig. 1 Structures of GRPR agonists [R-QWAVGHLM-NH_2] (**a**) and antagonists [R-fQWAVGHL-NHEt] (**b**) peptides. *FP* 2-fluoropropionate, *FB* 4-fluorobenzoate, *Aca* 5-amino caproic acid

HPLC. Identity and purity were established by LC/MS: FP-Aca-QWAVGHLM-NH_2 (m/z 1127.7 $[M + H]^+$, 97% purity), FP-fQWAVGHL-NHEthyl (m/z 1058.7 $[M + H]^+$, 95% purity), FB-aca-QWAVGHLM-NH2 (m/z 1175.6 $[M + H]^+$, 93% purity), FB-fQWAVGHL-NHEthyl (m/z 1106.6 $[M + H]^+$, 95% purity), FP-GGGRDN-QWAVGHLM-NH_2 (m/z 1571.1$[M + H]^+$, 94% purity), and FP-GGGRDN-fQWAVGHL-NHEt (m/z 1615.2 $[M + H]^+$, 94% purity). Stock solutions of the peptides were prepared in water at a concentration of 1 mg/mL.

Qualitative LC/MS

Waters LC–MS system (Waters, Milford, MA) was employed with an Acquity UPLC system coupled to the Waters Q-Tof Premier high-resolution mass spectrometer. An Acquity BEH Shield RP18 column (150 × 2.1 mm) was used for chromatography. Elution was achieved with a mixture of two components: solution A was composed of 2 mM ammonium formate, 0.1% formic acid, and 5% CH_3CN; solution B was composed of 2 mM ammonium formate and 0.1% formic acid in CH_3CN. The elution profile at 0.2 mL/min is: 100% (v:v) A and 0% B at initial; gradient 0–40% B over 15 min; isocratic elution at 40% B for an additional 3 min; 40–80% B over 2 min; re-equilibrated with A for an additional 4 min. The retention time for each compounds is listed in Table 1. The injection volume was 10 μL. The entire column elute was introduced into the Q-Tof mass spectrometer. Ion detection was achieved in ESI mode using a source capillary voltage of 3.5 kV, source temperature of 100°C, desolvation temperature of 200°C, cone gas flow of 50 L/h (N_2), and desolvation gas flow of 700 L/h (N_2).

Quantitative LC/MS

For quantitative analysis of peptides for cell internalization studies, the LC/MS system consisted of an Agilent 1200 autosampler, Agilent 1200 LC pump, and an AB/MDS Sciex 4000 Q TRAP (Life Technologies Corporation, Carlsbad, California). Separation was achieved on an Agilent RP18 column (1.8 μm, 100 × 4.6 mm) with gradient system at flow rate of 1.0 mL/min with the same solvent system described in the qualitative section. A gradient of 0% B for 3 min ramped to 50% B was utilized and isocratic elution at 50% B for an additional 4 min, 80% B for 2 min, and re-equilibrated with A for additional 1 min. Different combinations of multiple-reaction monitoring (MRM) and

Table 1 Proposed structures of the metabolites formed by rat hepatocytes and the molecular weight peaks (m/z) observed in positive ESI mass spectrometry

Name/ rentention time (min)	Structure	Metabolite 1	Metabolite 2	Metabolite 3
BBN/10.47	Aca-QWAVGHLM-NH_2 [M + H] 1053.6	Aca-QWAVGHLM-OH [M + H] 1054.1	Aca-QW-OH [M + H] 446.5 AVGHLM-NH_2 [M + H] 626.5	Aca-QWA-OH[M + H] 517.3 VGHLM-NH_2 [M + H] 555.4
NBBN/11.47	fQWAVGHL-NHEt [M + H] 984.4		fQW-OH [M + H] 480.3	fQWA-OH [M + H] 551.4 VGHL-NHEt [M + H] 452.4
FP-BBN/ 14.81	FP-aca-QWAVGHLM-NH_2 [M + H] 1127.8	FP-aca-QWAVGHLM-OH [M + H] 1128.8	FP-aca-QW-OH [M + H] 520.3 AVGHLM-NH_2 [M + H] 626.5	FP-aca-QWA-OH [M + H] 591.4 VGHLM-NH_2 [M + H] 555.4
FP-NBBN/ 17.56	FP-fQWAVGHL-NHEt [M + H] 1058.7		FP-fQW-OH [M + H] 554.4	FP-fQWA-OH [M + H] 625.4
FB-BBN/ 17.52	FB-aca-QWAVGHLM-NH_2 [M-H] 1173.9	FB-aca-QWAVGHLM-OH [M-H] 1174.9	FB-aca-QW-OH [M-H] 566.5	FB-aca-QWA-OH [M-H] 637.5
FB-NBBN/ 18.71	FB-fQWAVGHL-NHEt		FB-fQW-OH [M + H] 600.5	FB-fQWA-OH [M + H] 671.5
G-BBN/ 10.45	GGGRDN-QWAVGHLM-NH_2 [M + H] 1497.1	GGGRDN-QWAVGHLM-OH [M + H] 1498.1	AVGHLM-NH_2 [M + H] 626.5	VGHLM-NH_2 [M + H] 555.4
G-NBBN/ 11.85	GGGRDN-fQWAVGHL-NHEt [M + H] 1541.1		WAVGHL-NHEthy [M + H] 523.5	VGHL-NHEt [M + H] 452.4
FP-G-BBN/ 11.66	FP-GGGRDN-QWAVGHLM-NH_2 [M + H] 1571.1	FP-GGGRDN-QWAVGHLM-OH [M + H] 1572.1	FP-GGGRDN-QW-OH [M + H] 963.6 AVGHLM-NH_2 [M + H] 626.5	FP-GGGRDN-QWA-OH [M + H] 1034.7
FP-G-NBBN/ 13.11	FP-GGGRDN-fQWAVGHL-NHEt [M + H] 1615.2		FP-GGGRDN-fQW-OH [M + H] 1110.8	FP-GGGRDN-fQWA-OH [M + H] 1181.8

full scan MS/MS experiments were performed. Standards were prepared for each peptide covering the concentration range from 0.001 to 10 μM in 1:1 CH_3CN-water. Three replicate injections (10 μL) were made for each concentration level. The specific comparisons made for quantitation used a single MRM transition per analyte. [Aca-QWAVGHLM-NH_2 (527.3/110.1), fQWAVGHL-NHEt (551.3/120.1), GGGRDN-QWAVGHLM-NH_2 (749.1/110.1), GGGRDN-fQWAVGHL-NHEt (771.1/110.1), FP-Aca-QWAVGHLM-NH_2 (1128.6/110.1), FP-fQWAVGHL-NHEt (1059.5/110.1), FB-Aca-QWAVGHLM-NH_2 (1175.6/110.1), FB-fQWAVGHL-NHEt (1106.6/110.1), FP-GGGRDN-QWAVGHLM-NH_2 (786.0/110.1), and FP-GGGRDN-fQWAVGHL-NHEt (808.1/110.1)].

Incubation with hepatocytes to determine metabolic profile

Cryopreserved hepatocytes from male Sprague–Dawley rats (Celsis In Vitro Technologies, Inc., Baltimore, MD) were used for the in vitro metabolism studies. The cells, which were stored in liquid nitrogen (12–24 months), were thawed rapidly at 37°C in a water bath and gradually diluted with cell culture medium (Celsis In Vitro Technologies, Inc.). After washing the cells with the medium and adjusting the viable cell concentration to 1.0×10^6 cells per mL, the resulting cell suspension was incubated at 37°C for 15 min prior to the introduction of the test compound. The peptides were added to a 1.0 mL suspension of cells so as to achieve a final concentration of test compound of 10 μM. The suspension was maintained at 37°C. At various time points (10, 30, 60, 120, and 240 min), an aliquot (100 μL) of cell suspension was removed and added to 100 μL acetonitrile. This treatment resulted in cell lysis so that the metabolites analyzed could be either bound onto cell surface or internalized into the cells. Each aliquot was centrifuged at 5,000 rpm for 5 min. The supernatants (10 μL) were analyzed by LC–MS.

Internalization studies in PC-3 cell line

The PC-3 human prostate carcinoma cell line was purchased from American type culture collection (ATCC, Manassas, VA). PC-3 cells were grown in DMEM (Mediatech Inc., Manassas, VA) supplemented with 10% (v/v) fetal bovine serum (FBS) (Mediatech), 100 IU/mL penicillin, and 100 μg/mL streptomycin (Invitrogen, Carlsbad, CA), at 37°C in a humidified atmosphere containing 5% CO_2.

For the uptake assay, PC-3 cells were seeded into 6-well plates at a density of 1×10^6 cells per well and incubated for 24 h. Cells were rinsed three times with phosphate-buffered saline (PBS), followed by the addition of tested peptides to the cultured wells in triplicate (1 nmol/well). After incubation at 37°C for 15, 30, 60, and 120 min, the samples were processed in two different manners at each time point. For the first set, the media was collected for quantitative analysis of the unbound ligand. After washing twice with 1 mL saline, the cells were lysed by addition of 500 μL 0.1 N NaOH and then neutralized with 500 μL 0.1 N HCl. The final solution was collected for analysis of total cellular binding. In another set of plates, after the medium was separated, the cells were washed twice (0.5 mL) with 50 mM glycine and 0.1 M NaCl (pH 2.8). The acid washing buffer was collected since it contained the cell surface binding component. The cells were then lysed by adding 0.1 N NaOH and 0.1 N HCl and the resulting mixture was analyzed for internalized ligand. In total, four fractions were collected and analyzed by LC/MS, including unbound ligand, total bound ligand, cell surface binding ligand, and internalized ligand.

Results

Metabolism in rat hepatocytes

All agonist and antagonist peptides were incubated with the rat hepatocytes for metabolite analyses. All of the metabolites, whether intracellular or extracellular, were sampled by treating the aliquot of the cell suspension with CH_3CN to lyse the cells. The metabolites were analyzed by LC/MS and their structures were proposed based on the sequence of the individual peptide (Table 1). Both GRPR agonist (R-QWAVGHLM-NH_2) and antagonist (R-fQWAVGHL-NHEt) contain a homologous center of the sequence (WAVGHL). Consequently, the most common metabolites derived from all peptides resulted from peptide bond hydrolysis between W and A, which produced N-terminal sequences (R-QW-OH) for BBN (Fig. 2) and (R-fQW-OH) for NBBN. The peptides were also hydrolyzed between A and V, forming the amino terminal fragment R-QWA-OH and the carboxy terminal VGHLM-NH_2 (m/z 555) for the BBN peptides and R-fQWA-OH and VGHL-NHEt (m/z 452) for NBBN. The BBN peptides also derived a unique metabolite from hydrolysis of the C-terminal amide. The parent amide (R-QWAVGHLM-NH_2) exhibited a molecular ion [M + 1] that was 1 amu lower than that of its acid metabolite (R-QWAVGHLM-OH). The ability to conduct high-resolution mass measurements was important to allow the characterization of this metabolite.

The metabolic profile changed after addition of the sequence GGGRDN to the amino terminus. The metabolites of R-GGGRDN-fQWAVGHL-NHEt result from peptide bond hydrolysis between either D and N to generate a carboxyl terminal sequence N-fQWAVGHL-NHEt (m/z 1098.8) or between R and D to generate a carboxyl

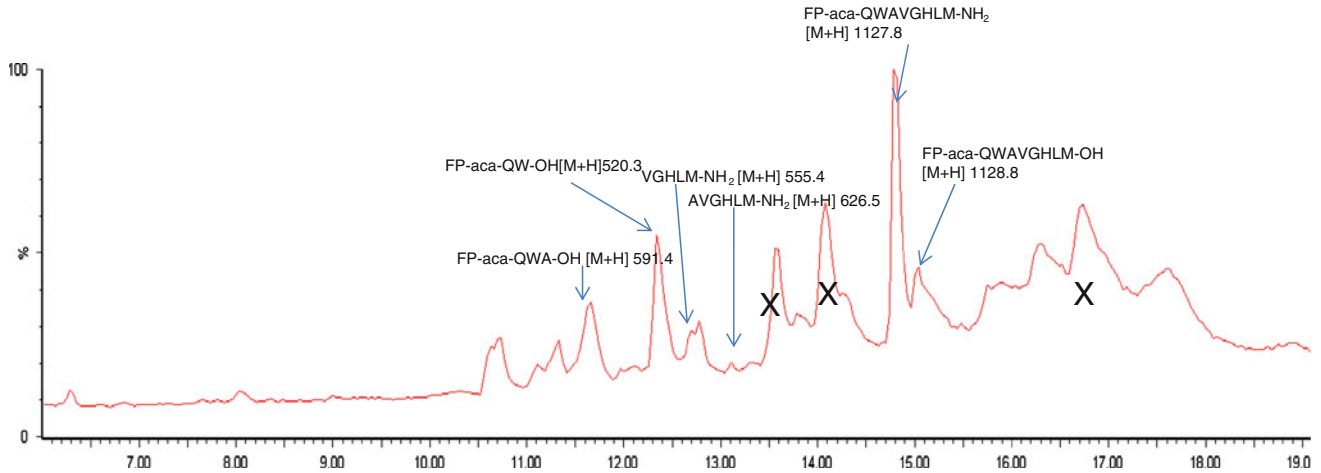

Fig. 2 The total ion chromatography (TIC) of agonist [FP-BBN] metabolites after 30 min of incubation in rat hepatocytes. Peaks labeled (X) were derived from the incubation media, which was confirmed by HPLC analysis of a blank

terminal sequence (DN-fQWAVGHL-NHEt) (m/z 1213.9). No hydrolysis of the ethylamide was observed.

The metabolic stability of the peptides was evaluated in the same preparation of rat hepatocytes, based on the rate of disappearance of the parent peptides. Within 2 h, the BBN peptides were almost undetectable from the assay solution, while the half-lives of parent peptides with rat hepatocytes for BBN, FP-BBN, FB-BBN, G-BBN and FP-G-BBN were estimated to be 4, 25, 3.8, 27 and 68 min, respectively (Fig. 3a). The NBBN peptides were more resistant to the hepatocytes. The half-life values of parent for NBBN, FP-NBBN, FB-NBBN, G-NBBN and FP-G-NBBN were estimated to be 32, 130, 37, 44, and 154 min, respectively (Fig. 3b).

Cell uptake and internalization

The highly sensitive 4000 Qtrap MS system was used to quantitate ligand binding and internalization with PC-3 cells. Standard curves of the instrument were established with various concentrations of the peptides in CH_3CN:water (1:1). A linear response was observed from 0.002–10.0 μM (0.02–100 pmol on column). The detection limit (s/n > 3) for most ligands was approximately 1 nM or less.

The direct binding study was performed by incubating the peptides with GRPR expressing PC-3 prostate cancer cells (Markwalder and Reubi 1999). At specified time points, aliquots were taken, processed as described in the methods section, and the various extracts quantitatively analyzed for parent peptide using LC/MS (Figs. 4, 5). We found that all ligands were more stable during PC-3 cell incubation compared with hepatocyte incubation. The proportion of parent compound exceeded 55% in all compartments (data not shown). Four components from each incubation were analyzed including unbound ligand

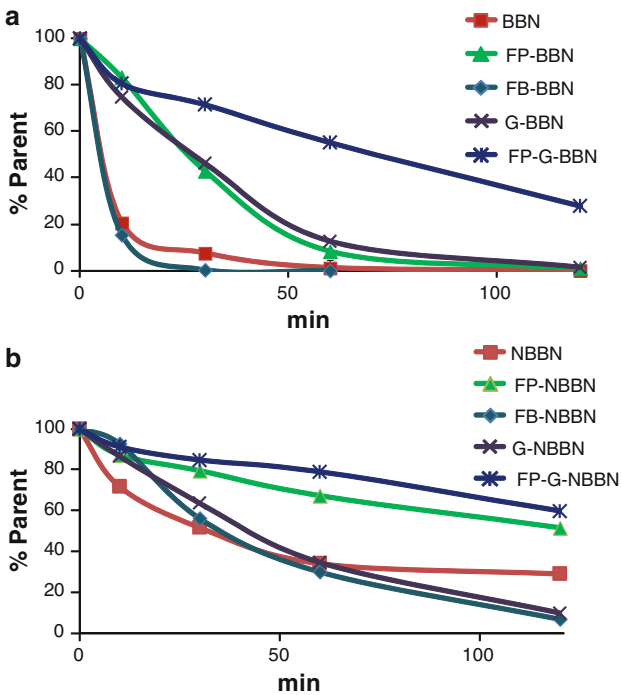

Fig. 3 **a** The metabolic rate of BBN, FP-BBN, FB-BBN, G-BBN and FP-G-BBN presented as the percent of parent ligand at various time points during 120 min of incubation with rat hepatocytes. **b** The metabolic rate of NBBN, FP-NBBN, FB-NBBN, G-NBBN and FP-G-NBBN presented as the percent of parent ligand at various time points during 120 min of incubation with rat hepatocytes

from the media, surface bound ligand from the acidic wash of the cells, internalized ligand from the lysed cells after acid wash and total surface bound and internalized ligand from lysed cells without acid wash. The cell uptake was expressed as the percent of total ligand added. Agonists (BBN, FP-BBN and FB-BBN) showed higher internalization with concomitantly lower surface binding while

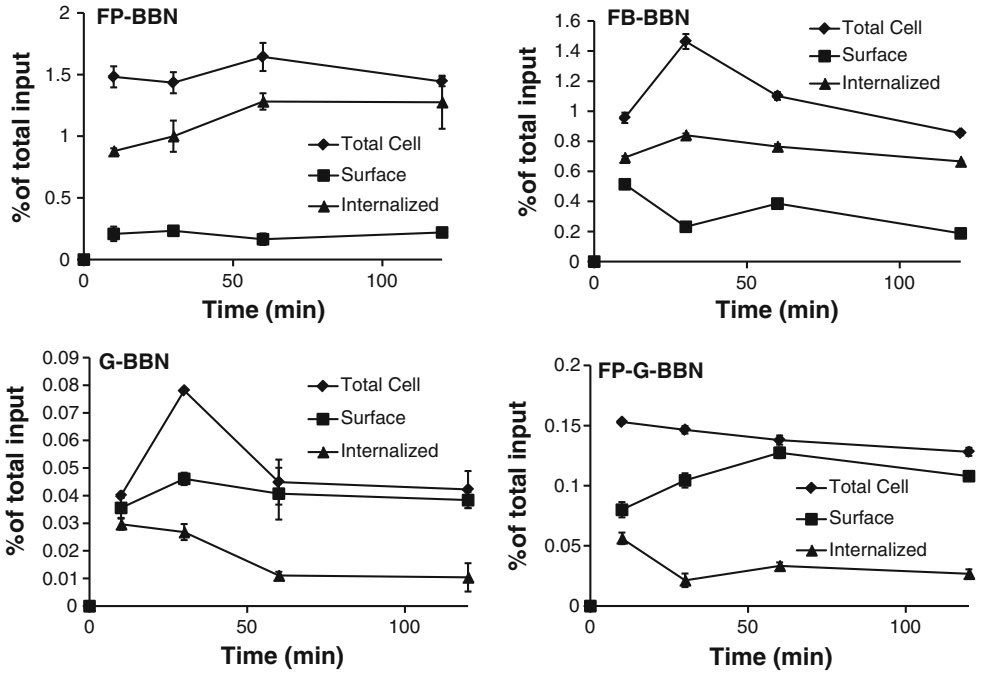

Fig. 4 The percent of parent ligand of FP-BBN, FB-BBN, G-BBN and FP-G-BBN observed in total cell binding, surface binding and internalization during 120 min of incubation in PC-3 cells

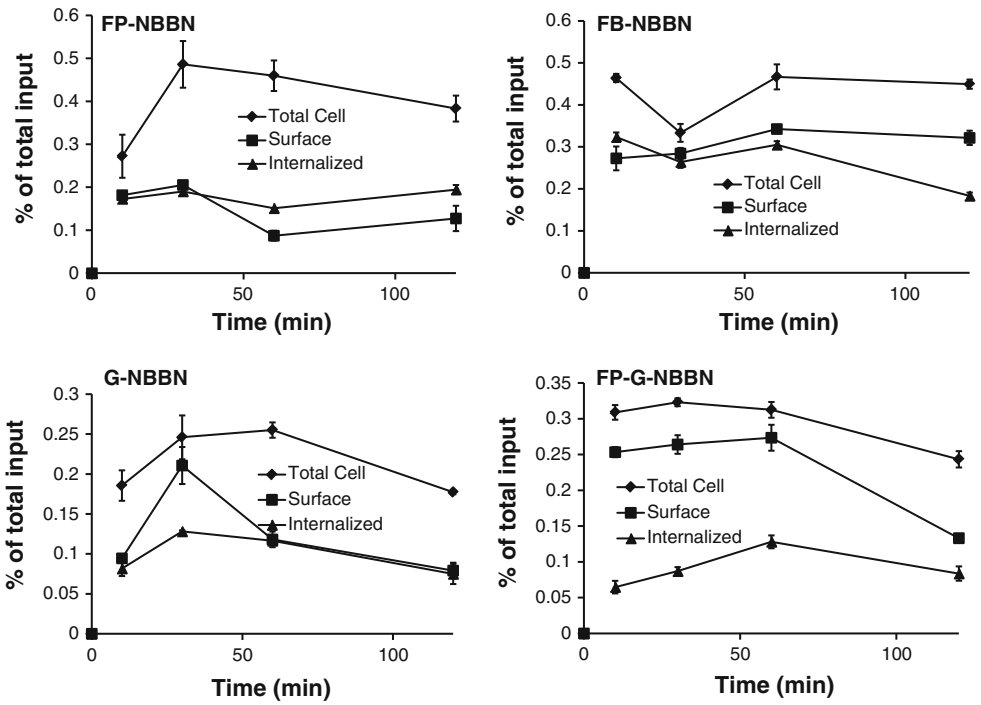

Fig. 5 The percent of parent ligand of labeled FP-NBBN, FB-NBBN, G-NBBN and FP-G-NBBN observed in total cell binding, surface binding and internalization during 120 min of incubation in PC-3 cells

antagonists (NBBN, FP-NBBN, FB-NBBN, G-NBBN and FP-G-NBBN) showed very low internalization compared with level of cell surface binding. The modified peptide G-BBN and its FP-derivative, FP-G-BBN, showed much lower total cell uptake compared with FP-BBN and FB-BBN.

Discussion

LC/MS is an efficient and sensitive method for screening radiotracer candidates for metabolic profile and tissue uptake without the need for radiolabeling (Ma et al. 2003). In this study, the LC/MS technique was used to evaluate

metabolism and internalization of several BBN derived ligands for GRPR. The method provides not only information for structural identification of metabolites but also highly selective, accurate quantitation of ligands in biological extracts.

BBN derived radiotracers are limited in their application to in vivo tumor imaging due to the rapid metabolism and poor stability. After incubation with rat hepatocytes, we found that analogs of the agonist (BBN) are metabolized more quickly than similar analogs of the antagonist (NBBN). Interestingly, the metabolic stability was enhanced by capping the amino terminus with FP, but not with FB. Both fluorine labeled BBN and NBBN were metabolized in a similar pathway to what had previously been elucidated (Linder et al. 2009). Metabolic proteolysis between the WA and AV was expected for the BBN derived peptides and this cleavage was observed for both agonist and antagonist peptides. In addition, all of the labeled BBN peptides showed hydrolysis of the C-terminal amide. The shorter half-life of the labeled BBN peptides could be attributed to the relatively rapid formation of the amide hydrolysis product, and the difference in peptide sequence compared to the antagonist. The differences in sequence between the two classes of peptides, a C-terminal methionine in the agonist and an N-terminal R-phenylalanine in the antagonist, could also influence the enzymatic hydrolysis. FP-G-BBN was metabolized slower than other fluorine-labeled BBN, which may result in better tumor imaging properties even though it exhibited lower in vitro PC-3 cell uptake.

We also used LC/MS to directly determine binding and internalization of various GRPR ligands to human prostate derived PC-3 cells. The agonist ligands exhibited two- to threefold higher total cell uptake than the antagonists. The increased cell uptake was due to higher internalization of agonists as the cell surface binding was very similar between the two groups of peptides. The antagonists displayed almost no internalization. As GRPR agonists, directly modified BBN (FP-BBN and FB-BBN) had similar cell uptake as compared to the unmodified agonist (BBN). However, FP-BBN was previously found to have better in vivo tumor imaging than FB-BBN presumably, because it was more polar and more slowly metabolized. It has been well established that introduction of PEG, sugar moiety, and oligo-glycine linkers could improve the in vivo kinetics of various peptides (Lee et al. 2010). Previously, we have also successfully used PEG and oligo-Glycine linkers to improve the pharmacokinetics of RGD peptides (Chen et al. 2004a; Liu et al. 2009b). The modified BBN with hydrophilic linker (GGGRDN-BBN and FP-GGGRDN-BBN) was found to have much lower PC-3 cell uptake in both surface and internalization. Meanwhile, the NBBN analogs (FP-NBBN, FB-NBBN, G-NBBN, FP-G-NBBN) were very similar with the unmodified antagonist NBBN which showed more efficient cell surface binding than internalization (Fig. 5).

Conclusion

The combination of LC and MS/MS can provide both structural information for identification of metabolites and accurate quantitation of ligands in cell binding experiments. The metabolism profiles of BBN derived GRPR agonist and antagonist peptides were identified by LC/MS. The major metabolites resulted from peptide bond hydrolysis between W and A in rat hepatocyte incubation. The antagonist peptides were more metabolically stable than the agonist peptides. The agonist ligands (BBN, FP-BBN and FB-BBN) had higher cell uptake in PC-3 cells due to high internalization. The addition of the hydrophilic linker reduced the cell uptake of the ligands G-BBN and FP-G-BBN by interrupting internalization. The optimal imaging agent will depend on the interplay of ligand metabolism, cellular uptake, and internalization in vivo.

Acknowledgment This project was supported by the Intramural Research Program of the National Institute of Biomedical Imaging and Bioengineering (NIBIB), National Institutes of Health (NIH) and the International Cooperative Program of the National Science Foundation of China (NSFC) (81028009).

References

Abd-Elgaliel WR, Gallazzi F, Garrison JC, Rold TL, Sieckman GL, Figueroa SD, Hoffman TJ, Lever SZ (2008) Design, synthesis, and biological evaluation of an antagonist-bombesin analogue as targeting vector. Bioconjug Chem 19:2040–2048

Abiraj K, Mansi R, Tamma ML, Forrer F, Cescato R, Reubi JC, Akyel KG, Maecke HR (2010) Tetraamine-derived bifunctional chelators for technetium-99 m labelling: synthesis, bioconjugation and evaluation as targeted SPECT imaging probes for GRP-receptor-positive tumours. Chemistry 16:2115–2124

Ananias HJ, Yu Z, Dierckx RA, van der Wiele C, Helfrich W, Wang F, Yan Y, Chen X, de Jong IJ, Elsinga PH (2011) 99mtechnetium-HYNIC(tricine/TPPTS)-Aca-bombesin(7–14) as a targeted imaging agent with microSPECT in a PC-3 prostate cancer xenograft model. Mol Pharm 8:1165–1173

Cescato R, Maina T, Nock B, Nikolopoulou A, Charalambidis D, Piccand V, Reubi JC (2008) Bombesin receptor antagonists may be preferable to agonists for tumor targeting. J Nucl Med 49:318–326

Chen X, Hou Y, Tohme M, Park R, Khankaldyyan V, Gonzales-Gomez I, Bading JR, Laug WE, Conti PS (2004a) Pegylated Arg-Gly-Asp peptide: ^{64}Cu labeling and PET imaging of brain tumor $\alpha v\beta 3$-integrin expression. J Nucl Med 45:1776–1783

Chen X, Park R, Hou Y, Tohme M, Shahinian AH, Bading JR, Conti PS (2004b) microPET and autoradiographic imaging of GRP receptor expression with ^{64}Cu-DOTA-[Lys3]bombesin in human prostate adenocarcinoma xenografts. J Nucl Med 45:1390–1397

Cornelio DB, Meurer L, Roesler R, Schwartsmann G (2007a) Gastrin-releasing peptide receptor expression in cervical cancer. Oncology 73:340–345

Cornelio DB, Roesler R, Schwartsmann G (2007b) Gastrin-releasing peptide receptor as a molecular target in experimental anticancer therapy. Ann Oncol 18:1457–1466

Fleischmann A, Waser B, Gebbers JO, Reubi JC (2005) Gastrin-releasing peptide receptors in normal and neoplastic human uterus: involvement of multiple tissue compartments. J Clin Endocrinol Metab 90:4722–4729

Fleischmann A, Waser B, Reubi JC (2007) Overexpression of gastrin-releasing peptide receptors in tumor-associated blood vessels of human ovarian neoplasms. Cell Oncol 29:421–433

Gu D, Ma Y, Niu G, Yan Y, Lang L, Aisa HA, Gao H, Kiesewetter DO, Chen X (2011) LC/MS evaluation of metabolism and membrane transport of bombesin peptides. Amino Acids 40:669–675

Gugger M, Reubi JC (1999) Gastrin-releasing peptide receptors in non-neoplastic and neoplastic human breast. Am J Pathol 155:2067–2076

Lee S, Xie J, Chen X (2010) Peptide-based probes for targeted molecular imaging. Biochemistry 49:1364–1376

Linder KE, Metcalfe E, Arunachalam T, Chen J, Eaton SM, Feng W, Fan H, Raju N, Cagnolini A, Lantry LE, Nunn AD, Swenson RE (2009) In vitro and in vivo metabolism of Lu-AMBA, a GRP-receptor binding compound, and the synthesis and characterization of its metabolites. Bioconjug Chem 20:1171–1178

Liu Z, Li ZB, Cao Q, Liu S, Wang F, Chen X (2009a) Small-animal PET of tumors with ^{64}Cu-labeled RGD-bombesin heterodimer. J Nucl Med 50:1168–1177

Liu Z, Niu G, Shi J, Liu S, Wang F, Chen X (2009b) ^{68}Ga-labeled cyclic RGD dimers with Gly3 and PEG4 linkers: promising agents for tumor integrin $\alpha v\beta 3$ PET imaging. Eur J Nucl Med Mol Imaging 36:947–957

Liu Z, Yan Y, Chin FT, Wang F, Chen X (2009c) Dual integrin and gastrin-releasing peptide receptor targeted tumor imaging using ^{18}F-labeled PEGylated RGD-bombesin heterodimer ^{18}F-FB-PEG3-Glu-RGD-BBN. J Med Chem 52:425–432

Ma Y, Kiesewetter D, Lang L, Eckelman WC (2003) Application of LC-MS to the analysis of new radiopharmaceuticals. Mol Imaging Biol 5:397–403

Ma Y, Lang L, Reyes L, Tokugawa J, Jagoda EM, Kiesewetter DO (2009) Application of highly sensitive UPLC-MS to determine biodistribution at tracer doses: validation with the 5-HT1A ligand [^{18}F]FPWAY. Nucl Med Biol 36:389–393

Mansi R, Wang X, Forrer F, Kneifel S, Tamma ML, Waser B, Cescato R, Reubi JC, Maecke HR (2009) Evaluation of a 1,4,7,10-tetraazacyclododecane-1,4,7,10-tetraacetic acid-conjugated bombesin-based radioantagonist for the labeling with single-photon emission computed tomography, positron emission tomography, and therapeutic radionuclides. Clin Cancer Res 15:5240–5249

Markwalder R, Reubi JC (1999) Gastrin-releasing peptide receptors in the human prostate: relation to neoplastic transformation. Cancer Res 59:1152–1159

Nock B, Nikolopoulou A, Chiotellis E, Loudos G, Maintas D, Reubi JC, Maina T (2003) [^{99m}Tc]Demobesin 1, a novel potent bombesin analogue for GRP receptor-targeted tumour imaging. Eur J Nucl Med Mol Imaging 30:247–258

Reubi JC, Korner M, Waser B, Mazzucchelli L, Guillou L (2004) High expression of peptide receptors as a novel target in gastrointestinal stromal tumours. Eur J Nucl Med Mol Imaging 31:803–810

Schroeder RP, van Weerden WM, Bangma C, Krenning EP, de Jong M (2009) Peptide receptor imaging of prostate cancer with radiolabelled bombesin analogues. Methods 48:200–204

Shi J, Jia B, Liu Z, Yang Z, Yu Z, Chen K, Chen X, Liu S, Wang F (2008) 99mTc-labeled bombesin(7–14)NH2 with favorable properties for SPECT imaging of colon cancer. Bioconjug Chem 19:1170–1178

Shipp MA, Tarr GE, Chen CY, Switzer SN, Hersh LB, Stein H, Sunday ME, Reinherz EL (1991) CD10/neutral endopeptidase 24.11 hydrolyzes bombesin-like peptides and regulates the growth of small cell carcinomas of the lung. Proc Natl Acad Sci USA 88:10662–10666

Smith CJ, Volkert WA, Hoffman TJ (2005) Radiolabeled peptide conjugates for targeting of the bombesin receptor superfamily subtypes. Nucl Med Biol 32:733–740

Sun B, Schally AV, Halmos G (2000) The presence of receptors for bombesin/GRP and mRNA for three receptor subtypes in human ovarian epithelial cancers. Regul Pept 90:77–84

Wagner JG (1979) Fundamentals of clinical pharmacokinetics. Drug Intelligence Publications, Hamilton

Yan Y, Chen K, Yang M, Sun X, Liu S, Chen X (2010) A new ^{18}F-labeled BBN-RGD peptide heterodimer with a symmetric linker for prostate cancer imaging. Amino Acids 41:439–447

Yang YS, Zhang X, Xiong Z, Chen X (2006) Comparative in vitro and in vivo evaluation of two 64Cu-labeled bombesin analogs in a mouse model of human prostate adenocarcinoma. Nucl Med Biol 33:371–380

Yang M, Gao H, Zhou Y, Ma Y, Quan Q, Lang L, Chen K, Niu G, Yan Y, Chen X (2011) ^{18}F-labeled GRPR agonists and antagonists: a comparative study in prostate cancer imaging. Theranostics 1:220–229

Zhang H, Chen J, Waldherr C, Hinni K, Waser B, Reubi JC, Maecke HR (2004) Synthesis and evaluation of bombesin derivatives on the basis of pan-bombesin peptides labeled with indium-111, lutetium-177, and yttrium-90 for targeting bombesin receptor-expressing tumors. Cancer Res 64:6707–6715

Zhang X, Cai W, Cao F, Schreibmann E, Wu Y, Wu JC, Xing L, Chen X (2006) ^{18}F-labeled bombesin analogs for targeting GRP receptor-expressing prostate cancer. J Nucl Med 47:492–501